

Increased cholinergic response in α -synuclein transgenic mice (h- α -synL62)

Magdalena König, Beata Berlin, Karima Schwab, Silke Frahm, Franz Theuring,
Claude M Wischik, Charles Robert Harrington, Gernot Riedel, and Jochen Klein

ACS Chem. Neurosci., **Just Accepted Manuscript** • DOI: 10.1021/acschemneuro.8b00274 • Publication Date (Web): 25 Sep 2018

Downloaded from <http://pubs.acs.org> on September 26, 2018

Just Accepted

“Just Accepted” manuscripts have been peer-reviewed and accepted for publication. They are posted online prior to technical editing, formatting for publication and author proofing. The American Chemical Society provides “Just Accepted” as a service to the research community to expedite the dissemination of scientific material as soon as possible after acceptance. “Just Accepted” manuscripts appear in full in PDF format accompanied by an HTML abstract. “Just Accepted” manuscripts have been fully peer reviewed, but should not be considered the official version of record. They are citable by the Digital Object Identifier (DOI®). “Just Accepted” is an optional service offered to authors. Therefore, the “Just Accepted” Web site may not include all articles that will be published in the journal. After a manuscript is technically edited and formatted, it will be removed from the “Just Accepted” Web site and published as an ASAP article. Note that technical editing may introduce minor changes to the manuscript text and/or graphics which could affect content, and all legal disclaimers and ethical guidelines that apply to the journal pertain. ACS cannot be held responsible for errors or consequences arising from the use of information contained in these “Just Accepted” manuscripts.

Increased cholinergic response in α -synuclein transgenic mice (h- α -synL62)

Magdalena König¹, Beata Berlin¹, Karima Schwab², Silke Frahm², Franz Theuring², Claude M Wischik^{3,4}, Charles R Harrington^{3,4}, Gernot Riedel⁵ and Jochen Klein^{1*}

¹*Department of Pharmacology, Biocenter N260, Max-von-Laue Str. 9, Goethe University Frankfurt, 60438 Frankfurt am Main*

²*Charite - Universitätsmedizin Berlin, corporate member of Freie Universität Berlin, Humboldt-Universität zu Berlin, and Berlin Institute of Health, Center for Cardiovascular Research, Institute of Pharmacology, Berlin, Germany*

³*School of Medicine, Medical Sciences and Nutrition, University of Aberdeen, Aberdeen, UK*

⁴*TauRx Therapeutics Ltd., Singapore 068805, Singapore*

⁵*Institute of Medical Sciences, University of Aberdeen, Aberdeen UK*

*corresponding author: klein@em.uni-frankfurt.de

Abstract: Pathological accumulation of misfolded α -synuclein (α -syn) in the brain plays a key role in the pathogenesis of Parkinson's disease, leading to neuronal dysfunction and motor disorders. The underlying mechanisms linking α -syn aggregations with neurotransmitter disturbance in Parkinson's brains are not well characterized. In the present study, we investigated transgenic mice expressing an aggregation-prone form of full-length human α -syn (h- α -synL62) linked to a signal sequence. These mice display dopamine depletion and progressive motor deficits. We detected accumulation of α -syn in cholinergic interneurons where they are colocalized with choline acetyltransferase. Using microdialysis, we measured acetylcholine levels in the striatum at baseline and during stimulation in the open field and with scopolamine. While no difference between wild-type and transgenic mice was detected in 3 month old mice, striatal acetylcholine levels at 9 months of age were significantly higher in transgenic mice. Concomitantly, high-affinity choline uptake was also increased while choline acetyltransferase and acetylcholine esterase activities were unchanged. The results suggest a disinhibition of acetylcholine release in α -syn transgenic mice.

Keywords: alpha-synuclein, acetylcholine, microdialysis, cholinergic interneurons, scopolamine, muscarinic receptors

Introduction

Parkinson's disease (PD) is a common neurodegenerative disorder in humans with typical motor symptoms such as bradykinesia, rigidity and tremor. The pathophysiological process in the brain is characterized by a high load of the protein α -syn, which gradually deposits to form intracellular aggregates and fibrils known as Lewy bodies and Lewy neurites.¹

The physiological function of α -syn is not fully understood, but there is clear evidence for it playing a role in vesicular function at the synaptic terminal.² Monomeric α -syn interacts with soluble N-ethylmaleimide-sensitive factor attachment protein receptor (SNARE) complexes, which are directly involved in vesicle fusion and exocytosis.³ Therefore, a change in the structure, due to oligomerization and aggregation, can

1
2
3 contribute to degenerative processes and altered synaptic function. Misfolded α -syn
4 is known to impair axonal transport,⁴ and increase neuroinflammation.⁵

5
6 It is proposed that motor symptoms in PD are caused by a progressive loss of
7 dopamine (DA) neurons projecting from the midbrain to the striatum and therefore
8 influence basal ganglia function.⁶ However, DA interacts with a variety of other
9 neurotransmitters to control motor behavior. It is well known that the balance
10 between acetylcholine (ACh) and DA in the striatum is necessary for normal motor
11 function. The striatum is composed mainly of GABAergic projection neurons (medium
12 spiny neurons, MSNs) and interneurons.⁷ Striatal cholinergic interneurons (ChIs)
13 represent only about 2% of the total striatal neuronal population,⁸ but have large
14 arborizing axonal varicosities within the striatum. This suggests that these neurons
15 may have an important role in modulating striatal activity.⁹ ChIs receive inputs from
16 cortical and thalamic glutamatergic neurons and from dopaminergic projections from
17 the Substantia Nigra pars Compacta (SNpC).¹⁰ Release of ACh from ChIs is
18 regulated by both dopaminergic receptors (D1/D5 and D2) and muscarinic ACh
19 receptors (M2/M4) on somatodendritic and axonal sites.¹¹ D2 receptors inhibit striatal
20 ACh efflux by lowering both synaptic activation and autonomous action potential
21 firing. D1 receptors are located mainly at the somatodendritic sites where they
22 depolarize the cell and enhance ACh release. The muscarinic M2/M4 receptors both
23 reduce ACh release by either reducing exocytosis on the axonal site or inducing
24 hyperpolarization on the somatodendritic site. DA depletion in the striatum can
25 therefore lead to a disturbed function of ChIs, contributing to the emergence of motor
26 symptoms.
27
28
29
30

31 Several genetic mouse models of PD have been developed that reflect many aspects
32 of the disease and the underlying mechanisms of α -syn pathology contributing to
33 motor symptoms and neurodegeneration.¹² Most of the transgenic synuclein models
34 overexpress human wild-type α -syn or α -syn carrying A53T or A30P mutations.¹²
35 Overexpression of α -syn has been shown to reduce dopamine release in transgenic
36 mice.¹³ However, not all α -syn-overexpressing transgenic mice form intracellular
37 inclusions or cell loss in the substantia nigra.¹⁴ The vulnerability of dopamine neurons
38 to α -syn overexpression has been well studied, but several reports have shown that
39 noradrenergic, serotonergic or cholinergic neurotransmitter systems are also
40 affected.¹⁵
41
42

43 We have recently reported on transgenic h- α -synL62 (L62) mice, which show high
44 levels of expression of human α -syn (h- α -syn); aggregates were already observed by
45 3 months of age.¹⁶ L62 showed a hypoactive phenotype and age progression was
46 associated with more severe impairments in motor activity and coordination. In
47 microdialysis experiments, a progressive lowering of amphetamine-induced
48 dopamine (DA) release in the striatum appeared in L62 between 3 and 9 months of
49 age.¹⁶ In the present study, we used h- α -synL62 mice at the age of 3 and 9 months
50 to investigate the impact of h- α -syn aggregation on cholinergic functions in the
51 striatum.
52
53

54 **Results and Discussion**

55
56 **Cholinergic neurons are affected by h- α -syn inclusions.** The pathologic hallmark
57 of PD is a degeneration of dopaminergic neurons of the Substantia nigra pars
58
59
60

compacta and of their striatal terminals. However, there are also reports of neuronal loss and alterations in cholinergic neurotransmission in the basal forebrain and in cortical structures.^{17,18} Cholinergic neurons are characterized by expression of the enzyme choline acetyltransferase (ChAT), which is localized to the soma and presynaptic endings. Alpha-synuclein plays a major role in the presynaptic cytoskeleton and accumulates specifically in presynaptic terminals. In histological staining experiments from L62, h- α -syn inclusions are pronounced in ChAT-positive neurons in several brain areas including striatum, olfactory nucleus, spinal cord and nucleus basalis magnocellularis (Fig. 1A) that are all known for their role in PD pathology. Cell counts of ChAT-positive neurons in the striatum confirmed a significant reduction of cells in L62 mice at 3 and 8 months of age relative to WT (Fig. 1B). Our results suggest that accumulation of h- α -syn in cholinergic neurons causes a loss of ChIs in the striatum, a brain region particularly important for the control of movements. These findings could be confirmed in another study with a model of widespread progressive synucleinopathy throughout the forebrain. Animals displayed progressive reduction in cortical and striatal ChAT positive interneurons, indicating that cholinergic interneurons may be more vulnerable to h- α -syn toxicity.¹⁹ However, in our model there is a lack of progression in the loss of ChAT positive neurons between 3 and 9 months of age. In L62 mice, h- α -syn aggregates reached their maximum aggregation state also with 3 months and showed no age progression in aggregation, but in severity of motor symptoms.¹⁶ Possibly there are other mechanisms, such as changes in neurotransmission, which contribute to the progression of motor symptoms.

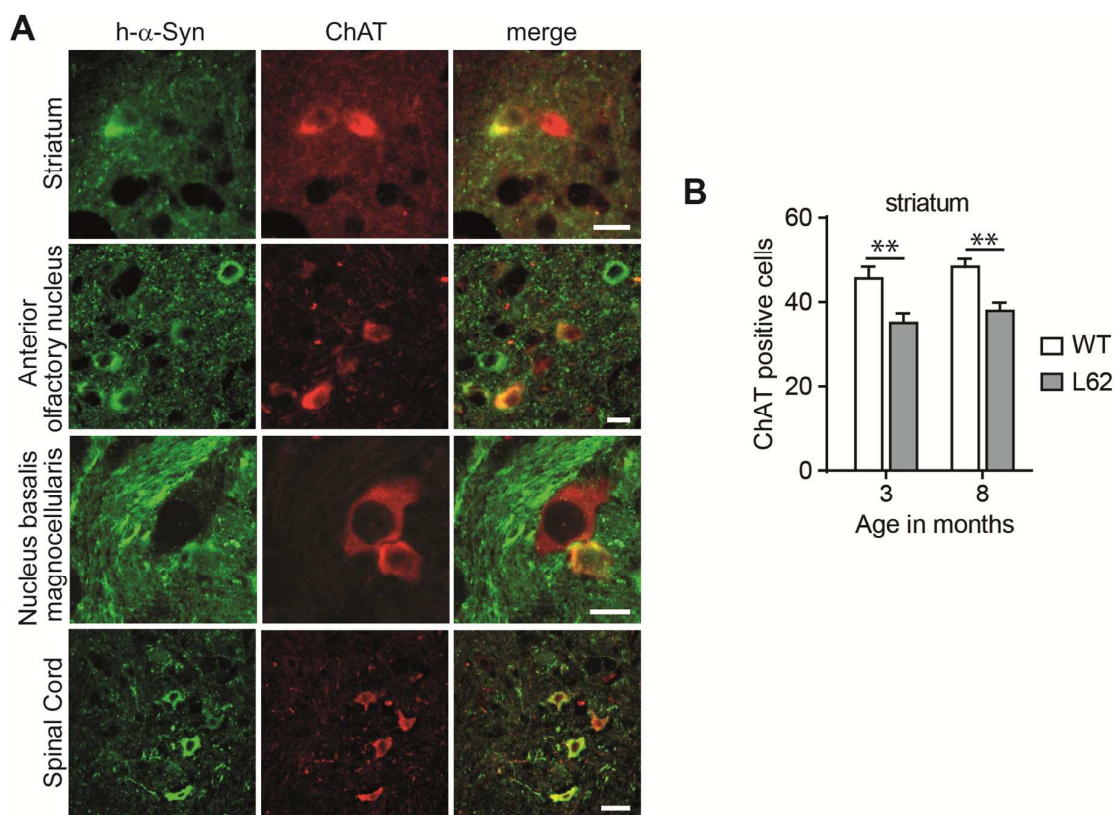


Figure 1: Cholinergic neurons are affected by h- α -syn inclusions in L62 mice. (A) A subset of cholinergic neurons, positive for ChAT (red), in the striatum, the olfactory

nucleus, the nucleus basalis magnocellularis and the spinal cord were also stained for h- α -syn (green) inclusions in L62 mice. The yellow color in the merged images indicates colocalization of ChAT and h- α -syn. Scale bars: 20 μ m. (B) Manual cell counting of striatal interneurons at Bregma 0.74 ± 0.25 revealed loss of striatal cholinergic interneurons in transgenic L62 compared to WT mice at 3 and 8 months of age. Values are given as mean \pm SEM (N = 8-12 mice per group). Statistics: two-way ANOVA for genotype and age as variables: Genotype $p < 0.0001$, age and interaction ns. Bonferroni posttest: **, $p < 0.01$ vs WT.

High-affinity choline uptake is upregulated in 9 months old transgenic mice. To gain a better understanding of the overall effects of h- α -syn on cholinergic synapses, the activity of three enzymes and transporters obligatory for ACh synthesis was measured (Fig. 2 A–C). ChAT is localized in presynaptic terminals and is responsible for the synthesis of ACh. When ChAT activities were determined, we found an age-dependent increase in ChAT activity ($p < 0.01$), but no genotype effect (Fig. 2A). Hence, ChAT activity was unchanged in spite of reduced cholinergic cell counts (Fig. 1B). However, ChAT activity is not limiting for ACh synthesis.

The activity of high-affinity choline uptake (HACU) reflects the transport of choline (Ch) back into the presynaptic compartment and is considered a rate-limiting step for the synthesis of ACh.²⁰ HACU activity is controlled by the presence of the choline transporter-1 (CHT-1) in the plasma membrane which is internalized depending on the neuronal firing rate.²¹ Hence, HACU measured *ex vivo* provides a measure of *in vivo* turnover of ACh prior to sacrifice.²² The activity of HACU in 9 month old mice was significantly greater for L62 mice relative to WT (Fig. 2B, $p = 0.02$). This suggests that degeneration of cholinergic cells in the striatum can lead to compensatory up-regulation of HACU activity which maintains cholinergic function. This finding is reminiscent of a study with mice, which were heterozygous for a null mutation in the ChAT gene. In these mice, ChAT activity was reduced by 50%, but brain ACh levels were normal due to an increased expression of CHT1.²³

Ex vivo-data of the activity of the acetylcholinesterase (AChE) reflect the rate of breakdown of ACh in the synaptic cleft because AChE terminates the action of ACh. There was no difference in AChE activity between the two mouse strains at 9 months of age (Fig. 2C). Hence, the rate of breakdown of ACh is not affected by h- α -syn.

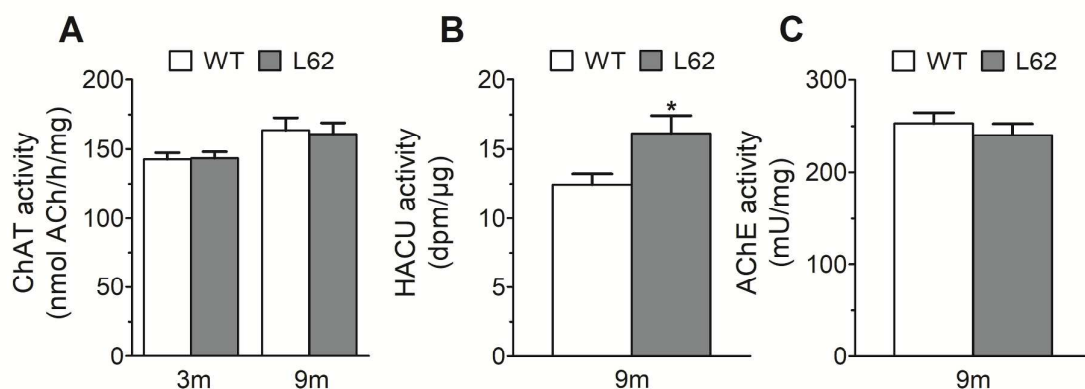


Figure 2. Activity of ChAT (A) in 3 and 9 month old mice, HACU (B) and AChE (C) in 9 month old mice. Data were obtained in hemibrain homogenates. Values are given

1
2
3 as mean \pm SEM (N = 6-10 mice per group). Statistics: two-way ANOVA for genotype
4 and age as variables: (A) Age $F_{1,36}=7.5$, $p < 0.01$, genotype and interaction ns. (B)
5 Student's t-test, two-tailed: $p=0.02$; (C) $p=0.48$.

6
7 **9 month old L62 mice display increased striatal ACh release during the open**
8 **field experiment.** To confirm a possible cholinergic phenotype caused by h- α -syn
9 accumulation, microdialysis measurements of the neurotransmitter ACh were
10 performed. The striatum was chosen as region of interest, since previous
11 experiments in L62 mice revealed that striatal dopamine levels are reduced in 9
12 month old mice upon amphetamine challenge (2 mg/kg). Baseline levels of DA in the
13 striatum of 9 month old WT and L62 mice were about 1 nM and during amphetamine
14 stimulation they increased 400% from baseline in WT and 250% from baseline in L62
15 mice.¹⁶ This difference in DA release was significant and shows that, despite of lack
16 of neuronal loss in the substantia nigra, striatal DA neurons are impaired in
17 transgenic L62 mice. As mentioned above, ChIs densely innervate the entire striatal
18 complex and receive input from extrinsic DA neurons of the mesencephalic
19 tegmentum.¹⁹ The output targets of the ChIs are the MSNs, which are important for
20 initiating and controlling movements.

21
22
23
24 Extracellular baseline concentrations of ACh were slightly higher in L62 but not
25 significantly different to WT at 3 and 9 months of age at the beginning of day 1
26 dialysis (Fig. 3A). The findings of baseline levels of ACh in the striatum are in
27 accordance with concentrations stated in the literature, which are about 1-5 nM.^{24,25}
28 In comparison to ACh, choline, the precursor of ACh, was lower in 9 month old mice,
29 an effect that was significant in L62 mice (Fig. 3B). This is possibly caused by an
30 increased turnover of ACh and heightened HACU activity of L62 mice at 9 months of
31 age (Fig. 2B), resulting in an increased uptake of extracellular choline into the
32 presynapse. It should be noted, however, that choline levels are much higher than
33 ACh levels, and choline metabolism mostly reflects phospholipid metabolism and not
34 ACh release.²⁰

35
36
37 When mice were placed into a novel environment (open field), ACh release was
38 stimulated by approx. 2-fold (Figs. 3C, D). This increase of ACh in the dorsal striatum
39 is probably due to motor activity during exploration in the open field.²⁶ There are no
40 data for open-field induced increases of ACh in the striatum of mice in the literature.
41 However, in experiments with Wistar rats, increased motor activity during the dark
42 phase of the rats' day-night cycle led to an increase in striatal ACh of 58%.²⁷

43
44
45 The time course in 3 month old mice was identical between L62 and WT (Fig. 3C). In
46 9 month old (Fig. 3D) mice, however, the movement stimulated rise in ACh was
47 higher in L62 mice during exploration and remained elevated over a longer period
48 after placing mice back into the home cage (two-way ANOVA: Genotype $F_{1, 22}=7.32$,
49 $p=0.01$). In similar experiments, Frahm et al. monitored the distance moved in an
50 open field, in which L62 mice showed a reduced activity¹⁶, but this was not recorded
51 here. Both reduced locomotor activity and elevated ACh levels can be explained by
52 an impaired regulation of firing of ChIs. Striatal cholinergic interneurons express both
53 D1 and D2 DA receptors.^{28,29} Dopamine modulates striatal cholinergic tone via both
54 excitatory and inhibitory actions. D2 receptor stimulation slows the discharge rate of
55 striatal ChIs by modulating sodium ion currents,³⁰ and inhibits striatal ACh release.³¹

Conversely, D1 receptor stimulation facilitates ACh release.³² Therefore, impairment in dopaminergic D2 receptor regulation of ChIs would explain an increased ACh release after stimulation.

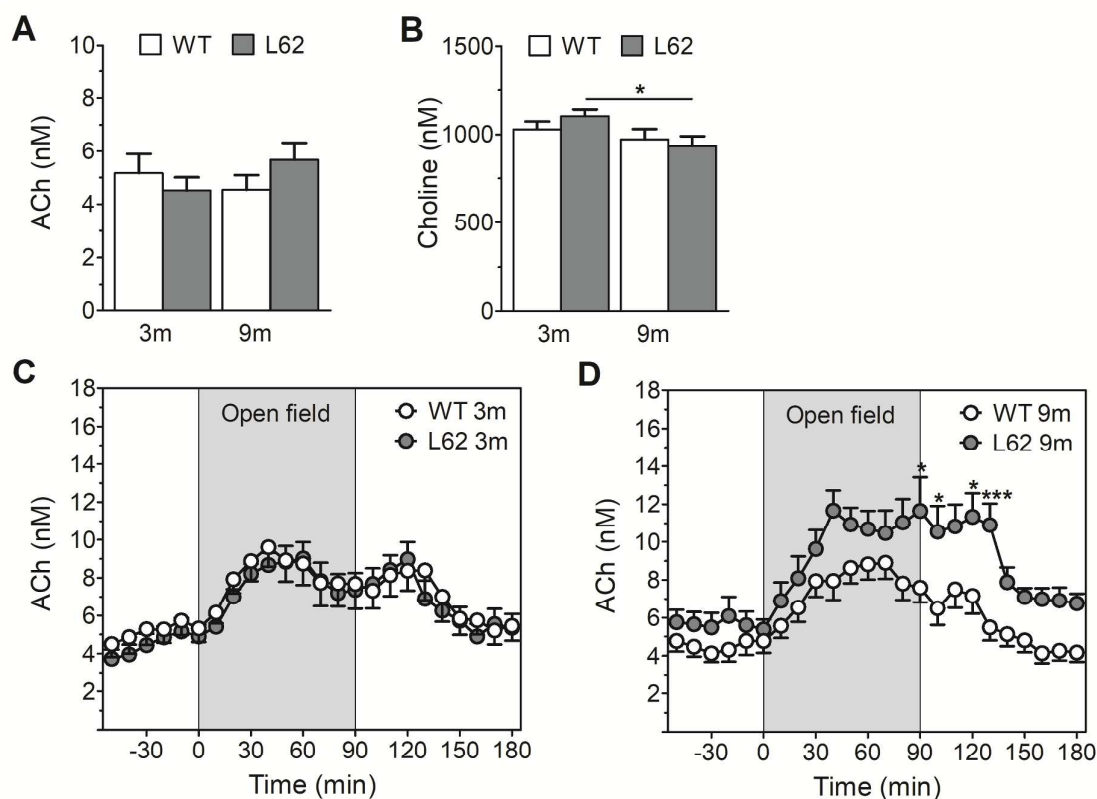


Figure 3. Baseline ACh and Ch levels before stimulation (A and B). Statistics: two-way ANOVA for genotype and age as variables: (A) Genotype, age and interaction ns. (B) Age $F_{1,53}=5.6$, $p=0.02$, genotype and interaction ns. Bonferroni post-test: *, $p<0.05$ vs L62. Extracellular striatal ACh levels in 3 and 9 month old mice before, during and after exposure to the open field (C and D). Statistics: two-way ANOVA for genotype and time as variables: (C) Time $F_{23,690}=20.47$, $p<0.0001$, genotype and interaction ns. (D) Time $F_{23,506}=22.35$, $p<0.0001$, genotype $F_{1,22}=7.32$, $p=0.01$, interaction $F_{23,506}= 2.25$, $p=0.0008$. Bonferroni post-test: *, $p<0.05$; **, $p<0.01$; ***, $p<0.001$ for L62 9m vs WT 9m. Values are presented as mean \pm SEM, derived from absolute values, not corrected for *in vitro* recovery (N=12-18 mice per group). Data for (A) and (B) were obtained for individual animals and averaged from 5-6 baseline samples for each mouse.

9 month old L62 mice display increased striatal ACh release during infusion of scopolamine. Besides DA receptors, muscarinic AChRs modulate the release of ACh in the striatum. ChIs express M2 and M4 receptors, which are present on the somatodendritic areas and the axon terminals.³³ At the somatodendritic site, mAChR are proposed to inhibit striatal ChIs by inducing hyperpolarization mediated by an outward K^+ current. mAChRs on the axon terminals cause presynaptic autoinhibition of ACh release by modulating K^+ and Ca^{2+} channels.³⁴ Scopolamine acts as a muscarinic antagonist; it blocks inhibitory M2/M4 receptors and causes an increase of extracellular ACh.³⁵ In 3 month old mice, scopolamine led to a 3-fold increase of

ACh in both lines (Fig 4C). In 9 month old mice (Fig. 4D), however, L62 mice displayed much higher increases in extracellular ACh levels than wild-type mice ($p < 0.01$). Most likely, the amplified effect of scopolamine in L62 mice can be explained by a disinhibition of ChIs in the striatum due to DA depletion and loss of inhibition by D2 receptors. Furthermore, DA denervation has been shown previously to reduce M4 mRNA which resulted in a loss of negative feedback inhibition and increased ACh release and turnover.³⁶ This mechanism may explain the small but significant increase of basal ACh in L62 vs. wild-type mice before scopolamine infusion (Fig. 4A). This increase in baseline levels of ACh is also reflected in the increased HACU activity measured in 9 month old mice (Fig. 2B).

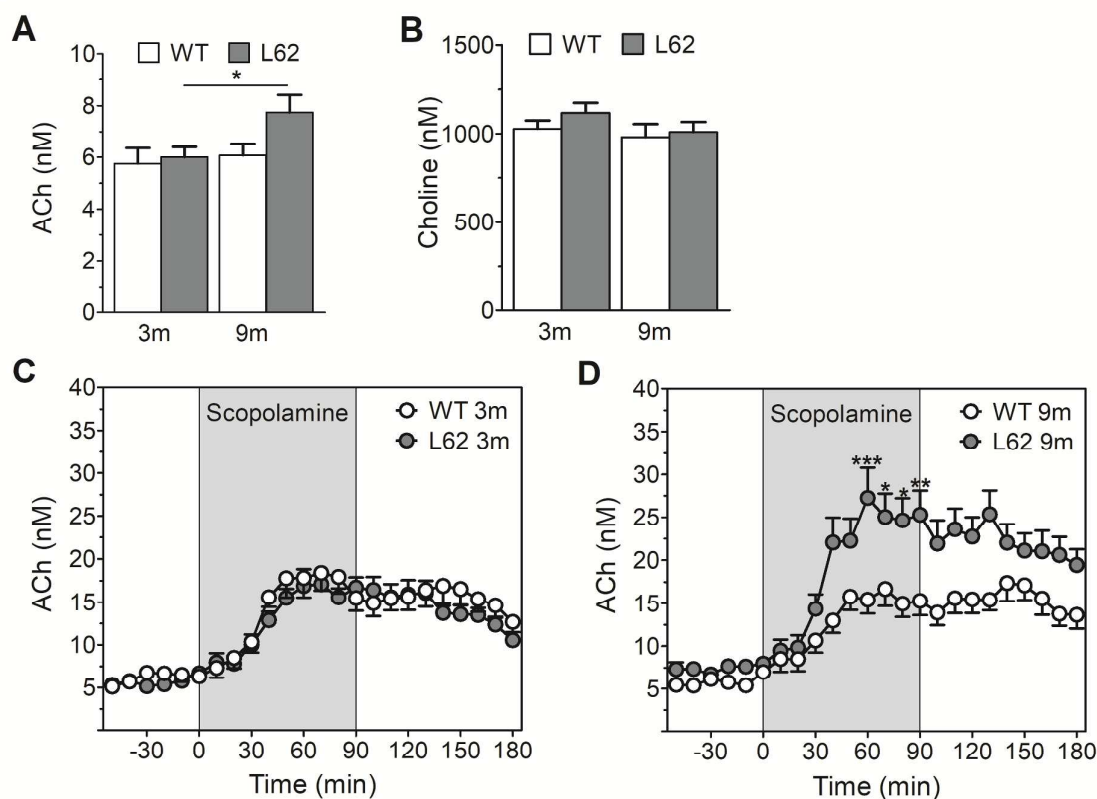


Figure 4. Baseline ACh and Ch levels before stimulation (A and B). Statistics: two-way ANOVA for genotype and age as variables: (A) Genotype $F_{1, 54} = 3.06$, $p = 0.09$, age $F_{1, 54} = 3.5$, $p = 0.07$, interaction ns. Bonferroni post-test: *, $p < 0.05$ vs L62. (B) Genotype, age and interaction ns. Extracellular striatal ACh levels in 3 and 9 month old mice before, during and after scopolamine exposure (shaded area) (C and D). Statistics: two-way ANOVA for genotype and time as variables: (C) Genotype, time and interaction ns. (D) Genotype $F_{1, 24} = 8.69$, $p = 0.007$, time $F_{23, 552} = 36.13$, $p < 0.0001$, interaction $F_{23, 552} = 3.19$, $p < 0.0001$. Bonferroni post-test: *, $p < 0.05$; **, $p < 0.01$; ***, $p < 0.001$ for L62 9m vs WT 9m. Values are presented as mean \pm SEM, derived from absolute values, not corrected for *in vitro* recovery (N = 12-18 mice per group). Data for (A) and (B) were obtained from individual animals and averaged from 5-6 baseline samples for each mouse.

Collectively, our results show that L62 at 9 months of age display higher striatal ACh release from challenged ChIs. The difference in extracellular ACh release seems to

1
2
3 be independent of the impact of α -syn on ChAT neurons in the striatum. Although
4 there is a reduction in ChAT positive cells in L62 mice, the cell counts did not decline
5 with age. Furthermore, there was no change in the activity of ChAT. There is
6 evidence that both phosphorylation and dephosphorylation of ChAT can alter its
7 catalytic activity and thereby regulate ACh synthesis.³⁷ α -syn may also have a
8 chaperone-like function and transgenic overexpression of this protein can lead to
9 changes in phosphorylation of ChAT.³⁸ However, it is generally considered, that the
10 activity of the high affinity choline transporter (HACU) is the rate-limiting step in ACh
11 synthesis and release, and measurements confirmed an increased activity of HACU
12 in L62 mice.
13
14

15 We suggest that the impairment of dopamine neurons leads to a disturbance in the
16 normal DA-ACh balance and that the increased cholinergic activity in this model may
17 arise from the reduced inhibition of dopaminergic neurons ending upon cholinergic
18 cells in the dorsal striatum.³⁹ The plastic alterations of striatal cholinergic
19 interneurons by DA denervation have never been investigated in α -syn
20 overexpressing mouse models. A change in activity of ChIs might have
21 consequences on movement and contribute to the progression of motor symptoms in
22 PD.
23
24

25 **Glucose and lactate levels increase in the open field but not during**
26 **scopolamine challenge.** Brains of PD patients showed glucose hypometabolism,⁴⁰
27 and α -syn aggregation in transgenic mouse models led to mitochondrial
28 dysfunction.⁴¹ We investigated the influence of α -syn aggregation on brain energy
29 metabolism by measuring extracellular glucose and lactate levels in microdialysate of
30 L62 and WT mice. Results were obtained from 3-4 consecutive baseline samples,
31 and 3-4 consecutive samples after placing mice into the open field and stimulating
32 with scopolamine, respectively.
33
34
35
36
37
38
39
40
41
42
43
44
45
46
47
48
49
50
51
52
53
54
55
56
57
58
59
60

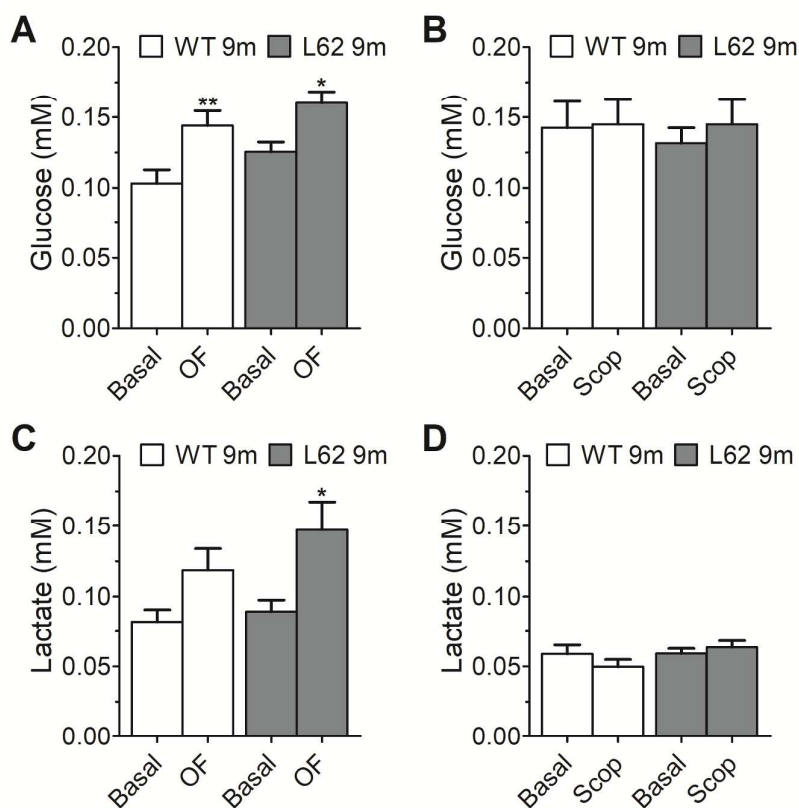


Figure 5: Glucose levels on day 1 (A) and day 2 (B) and lactate levels on day 1 (C) and day 2 (D) in 9 month old mice before and after stimulation measured in microdialysates. Statistics: two-way ANOVA for genotype and challenge as variables: (A) Genotype $F_{1,40} = 4.7$, $p = 0.04$, challenge $F_{1,40} = 18.15$, $p = 0.0001$, interaction ns. Bonferroni post-test: **, $p < 0.01$ vs WT, *, $p < 0.05$ vs L62. (B) Genotype, challenge and interaction ns. (C) Challenge $F_{1,28} = 14.03$, $p = 0.0008$, genotype and interaction ns. Bonferroni post-test: *, $p < 0.05$ vs L62. (D) Genotype, challenge and interaction ns. Values are presented as means \pm SEM. Data were obtained from individual animals and averaged from 3-4 consecutive samples. (A/C) $N = 9-11$, (B/D) $N = 8-9$ mice per group.

Glucose is the standard fuel for brain energy production and a precursor of ACh synthesis. It is taken into cholinergic presynaptic terminals and transformed into acetyl-Coenzyme A, which is used subsequently to synthesize ACh. ACh levels depend on glucose oxidation in periods of increased cholinergic activity.⁴² Extracellular glucose levels reflect a balance between supply from the blood and uptake into neurons. Behavioral stimulation in the open field caused glucose levels to increase, likely indicating an increased flux of glucose from blood during motor activity (Fig. 5A). Blood glucose, blood flow, and glucose uptake in the brain are coupled,⁴³ and thus an increase of glucose can reflect an increase of blood sugar or of blood flow in the striatum. Glucose levels were slightly greater in L62 at baseline (Fig. 5A), but the extent of glucose mobilization in the open field was almost identical in WT and L62 mice indicating that h- α -syn does not cause a generalised impairment in the ability of the brain to respond adequately to a physiological stimulus. Scopolamine perfusion did not change glucose levels in either WT or L62 (Fig. 5B).

1
2
3 In the absence of ischemia, extracellular lactate concentrations in the brain reflect
4 formation by astrocytes which support neuronal function in periods of high neuronal
5 demand.⁴⁴ Increase of ACh during the open field correlates with higher neuronal
6 activity shown by lactate increases in both L62 and WT to a similar extent (Fig. 5C).
7 Lactate levels in L62 mice were slightly higher in the open field experiment, which
8 may be explained by increased firing of the ChIs (Fig. 5C, Bonferroni posttest: *: $p <$
9 0.05 vs L62). Mice did not respond with an increase of lactate during stimulation with
10 scopolamine (Fig. 5D), probably because scopolamine blocks cholinergic excitation
11 of downstream neurons.
12

13 14 **Conclusion**

15
16 In this study we investigated the cholinergic system in the striatum in a mouse model
17 of synucleinopathy. L62 mice at 9 months of age displayed a cholinergic phenotype
18 which was characterized by strong increases of acetylcholine levels under stimulated
19 conditions, i.e. in the open field and during scopolamine perfusion. Direct effects of
20 synuclein on ChI are possibly due to the co-localization of h- α -syn and ChAT in
21 striatal cholinergic interneurons. However, the presynaptic function of cholinergic
22 interneurons does not seem to be affected by α -syn, as ChAT, HACU and AChE
23 activities are not reduced. In fact, although ChAT positive cells were reduced in the
24 striatum, the total activity of ChAT was unchanged and HACU showed an increased
25 activity, evidently to maintain the cholinergic function of the synapses. Glucose and
26 lactate responded normally, but the higher concentrations of lactate in L62 seen
27 during locomotor activity are in agreement with a greater neuronal activity during
28 exploration, which is proposed to be due to a disinhibition of cholinergic interneurons.
29
30

31 32 **Methods**

33
34 **Chemicals.** Neostigmine bromide, scopolamine and chemicals for the artificial
35 cerebrospinal fluid (aCSF) were purchased from Sigma-Aldrich (Munich, Germany).
36 The chemicals for the mobile phase of the HPLC analysis were obtained from Merck,
37 Darmstadt, Germany (KHCO_3), from VWR, Darmstadt, Germany (EDTA-2Na), from
38 Alfa Aesar, Karlsruhe, Germany (sodium decane-1-sulfonate) and from Sigma-
39 Aldrich, Munich, Germany (RotisolV HPLC grade water). Chemicals for AChE, ChAT
40 and HACU assays were purchased from Biotrend, Köln, Germany ($[^3\text{H}]$ -choline, $[^3\text{H}]$ -
41 acetyl coenzyme A), Sigma-Aldrich, Munich, Germany (acetylthiocholine iodide,
42 dithionitrobenzoic acid, Triton X-100, tetraisopropyl pyrophosphoramidate,
43 hemicholinium-3 and sodium tetraphenylboron) and from Merck, Darmstadt,
44 Germany (HEPES sodium salt). CMA 600 Microdialysis analyser reagents (Glucose,
45 Lactate and Calibrator reagents) were obtained from M Dialysis AB, Stockholm,
46 Sweden.
47
48

49
50 **Animals.** Transgenic mice were generated by GenOway (Lyon, France). Mice were
51 previously described and characterized by Frahm et al.¹⁶ They were bred in the
52 University facility of Charite Berlin and shipped by truck to the animal house in
53 Frankfurt. After delivery of the mice they were habituated to the animal facilities for at
54 least two weeks. Male and female homozygous L62 mice and WT litters were housed
55 in small colonies in a facility with controlled temperature and humidity and a day/night
56 cycle of 12/12 h. They had free access to food and water. All experiments were done
57
58
59
60

1
2
3 according to the German Law for Animal Protection (Tierschutzgesetz) and the
4 European Community Directive 63/2010/EU.

5
6 **ChAT-h- α -syn double labeling and ChI counting.** Formalin-fixed brain tissue was
7 embedded in paraffin, cut into 5- μ m coronal sections, deparaffinised and boiled in
8 10mM citric buffer.

9
10 For immunofluorescence, sections were blocked for 1 h in incubation buffer ((5% v/v)
11 normal goat serum in PBS containing 0.3% (v/v) Triton X-100) and incubated
12 overnight at 4° C in a primary antibody cocktail of mAb 204 (Santa Cruz
13 Biotechnology USA, diluted 1:200) and ChAT (H-95, Santa Cruz Biotechnology USA,
14 diluted 1:200), diluted in incubation buffer. The next day sections were incubated for
15 1.5 h with fluorochrome-conjugated secondary antibodies (Alexa Fluor® 488-
16 conjugated donkey anti-mouse IgG and Alexa Fluor® 568-conjugated goat anti-rabbit
17 IgG, Life Technologies, USA; both diluted 1:500 in incubation buffer) and examined
18 using a microscope equipped for fluorescence (Carl Zeiss, Germany).

19
20
21 For immunohistochemistry, sections were incubated in 0.3% (v/v) hydrogen
22 peroxidase solution and blocked for 20 min in blocking buffer (0.1% w/v BSA in PBS).
23 Afterwards, ChAT antibody (H-95, diluted 1:50) was added, followed by incubation
24 with corresponding biotinylated secondary antibody diluted 1:100 (Dako, Denmark).
25 Sections were developed with diaminobenzidine solution (Dako, Denmark),
26 counterstained with Ehrlich haematoxylin solution (Carl Roth, Germany), embedded
27 in Neo-Mount® (Merck Millipore, Germany) and images taken using a light
28 microscope (Carl Zeiss, Jena, Germany). Primary and secondary antibodies were
29 diluted in blocking buffer. Cholinergic interneurons were counted manually for the
30 entire striatum at Bregma +0.74 \pm 0.25 mm (according to Franklin and Paxinos)⁴⁵ for
31 3 consecutive brain sections. The mean value for each animal was used for
32 analyses.

33
34
35 **Activity of cholinergic enzymes and transporters.** Brain hemispheres were
36 homogenized with a 10-fold volume of isotonic HEPES-sucrose buffer (HEPES
37 sodium salt 10 mM, Sucrose 0.32 M, pH 7.4) using a tissue grinder (Potter S, B.
38 Braun, Melsungen, Germany) at 800 rpm and 15 strokes.

39
40
41 ChAT was measured by a modification of the Fonnum method.⁴⁶ Brain homogenate
42 containing 0.5 mg/ml protein was added to a total volume of 250 μ l reaction mix
43 (0.5% Triton X-100, 0.3 M NaCl, 0.02 M EDTA, 0.05 M Na₃PO₄ pH 7.4, 2 mM choline
44 chloride, 1 mM neostigmine bromide, 0.5 mCi [³H]-acetyl coenzyme A). Following
45 incubation at 37°C for 15 min, the reaction was stopped by addition of 250 μ l ice-cold
46 phosphate buffer (1 mM, pH 7.4). ACh was extracted with 1 ml 0.5 % sodium
47 tetraphenylboron in 85% toluene-15% acetonitrile. After centrifugation, aliquots of 0.8
48 ml were used for tritium quantification with a scintillation counter (Wallac system
49 1409, Perkin Elmer). ChAT activity was expressed as nmol of ACh formed per hour
50 per mg of protein (nmol/h/mg). Blank values were obtained by omitting the brain
51 homogenate.

52
53
54 HACU activity was determined in synaptosomal (P2) fractions obtained from one
55 hemisphere as previously described.⁴⁷ Brain hemispheres were homogenized in 10
56 mM HEPES-sucrose solution and centrifuged at 1,000 g for 10 min at 4°C and, the
57
58
59
60

1
2
3 resulting supernatant centrifuged again at 17,000 g for 10 min. The pellets from the
4 last centrifugation step (P2 fraction, containing the synaptosomes) were used for
5 HACU determination. Aliquots were incubated at 30°C in the presence of 0.5 μ M
6 [3H]-choline (diluted to 0.5 Ci/mmol; Biotrend, Cologne, Germany) in Krebs-Henseleit
7 buffer (KHB; containing NaCl 115 mM, KCl 7.1 mM, CaCl₂ 1.2 mM, MgSO₄ 1.2 mM,
8 NaHCO₃ 25 mM, Na₂HPO₄ 1.5 mM, glucose 12.8 mM, and saturated with carbogen
9 adjusting to pH 7.2-7.4). Incubations were done both, in the presence and absence of
10 1 μ M hemicholinium-3 (HC-3). Choline uptake was stopped after 5 min by placing the
11 reaction mix on ice and by adding ice-cold KHB. After three centrifugation steps
12 (14,000 g, 10 min) and washing with KHB buffer, the pellets were solubilized in 0.5 ml
13 methanol and 4 ml scintillation fluid (IRGA-SAFE PLUS, Perkin Elmer) and used for
14 tritium quantification by liquid scintillation counting. The HC-3-sensitive, high-affinity
15 choline uptake was calculated as the difference between uptake in the absence and
16 presence of HC-3 and expressed as dpm/mg protein. Protein content was
17 determined by the Bradford method.
18
19

20
21 AChE activity was measured by a modified Ellman method.^{48,49} Brain homogenate
22 (50 μ l) was mixed with 0.5% Triton X-100 (Sigma-Aldrich, Munich, Germany) to
23 dissolve membranes. Samples were centrifuged for 10 min. at 12,000 g and 4°C. 10
24 μ l of the supernatant was mixed with Ellman buffer and iso-OMPA (final
25 concentration 100 μ M). Acetylthiocholine and dithionitrobenzoic acid (1 mM and 500
26 μ M final concentrations, respectively) were added before measuring the absorbance
27 at 405 nm using a Victor multi-label plate reader (Perkin Elmer, Bedford, USA).
28 Enzyme activity was calculated using a standard curve prepared with each assay and
29 expressed in relation to protein amount (mU/mg protein). Protein determination was
30 carried out using the Bradford method.⁵⁰
31
32

33 **Probe implantation.** Self-made, I-shaped, concentric dialysis probes with an
34 exchange length of 2 mm and a molecular cut-off of 10,000 Da were constructed as
35 previously described.⁵¹ The in vitro recovery of the self-built probes amounted to 18.5
36 \pm 2.7 % for ACh and 23.2 \pm 2.8 % for Ch. After at least one week of acclimatization to
37 the housing conditions, the microdialysis probes were implanted. Mice were
38 anaesthetized with isoflurane (Forene®, Abbvie, Ludwigshafen, Germany) in
39 concentrations (v/v) of 4% isoflurane in air for induction and 1.5-2% isoflurane for
40 maintenance of anesthesia by a vaporisator (Kent Scientific, USA). The skull was
41 exposed and a small hole was drilled in the skull of one hemisphere. By means of a
42 stereotaxic apparatus (Stoelting, Chicago, USA), the probes were implanted into the
43 dorsal striatum using the following coordinates from bregma: AP: +0.5 mm, L: +2.2
44 mm, DV: -2.3 mm, according to the atlas of Franklin and Paxinos.⁴⁵ Glass ionomer
45 eluting cement (Micron® i-Cem, PrevestDenPro, Heidelberg, Germany) was used to
46 fix the implanted probe on the skull. All animals were allowed to recover at least 18
47 hours after surgery before starting the microdialysis experiments.
48
49
50

51 **In vivo microdialysis procedures.** Microdialysis experiments were carried out for
52 two consecutive days after probe implantation. Artificial cerebrospinal fluid (aCSF;
53 147 mM NaCl, 4 mM KCl, 1.2 mM CaCl₂, 1.2 mM MgCl₂) was pumped through the
54 probe at a constant rate of 2 μ l/min with a microinjection pump. Dialysate samples
55 (20 μ l) were collected every 10 min and immediately stored on ice. After collection,
56 samples were frozen at -80°C until analysis. For detection of extracellular ACh,
57
58
59
60

1
2
3 neostigmine (0.1 μM) was added to the perfusion liquid to stabilize basal extracellular
4 ACh levels for the following stimulating experiments. On day one of microdialysis,
5 after collection of basal levels for 60 min, mice were placed in a novel environment
6 (open field box, 35x32x20 cm) for 90 min to physiologically stimulate the ACh release
7 due to exploration and increased locomotor activity. After the open field stimulation,
8 mice were placed back into their home cage and dialysis was continued for another
9 90 min. On day two, baseline levels were collected for 60 min and then scopolamine
10 (1 μM) was infused for 90 min through the microdialysis probe to increase ACh
11 release pharmacologically. After stimulation, dialysis was continued without
12 scopolamine for another 90 min. Subsequently, mice were sacrificed and brains were
13 sectioned to verify the correct location of the probe in the dorsal striatum. The
14 hemisphere without probe implantation was used to prepare homogenates (see
15 above) for the measurement of acetylcholinesterase (AChE) activity, choline
16 acetyltransferase (ChAT) activity and high-affinity choline uptake (HACU).
17
18

19
20 **Determination of Acetylcholine, Choline, Glucose and Lactate.** ACh and choline
21 (Ch) were analyzed by directly injecting dialysates into a high performance liquid
22 chromatography (HPLC) system (Eicom HTEC-500, Kyoto, Japan) consisting of
23 degasser, low-speed pump, pre- and separation column, enzyme reactor carrying
24 immobilized AChE and choline oxidase, and an electrochemical detector with a
25 platinum electrode operating at 500 mV relative to an Ag/AgCl reference electrode.
26 The mobile phase contained 50 mM KHCO_3 , 134 μM Na_2EDTA , and 1.6 mM sodium
27 decane-1-sulfonate dissolved in RotisoIV® HPLC gradient water (pH 8.4). The flow
28 rate was set to 150 $\mu\text{l}/\text{min}$ and the injection volume was 10 μl . In this condition the
29 sensitivity of the assay for ACh is about 1-3 fmol per sample. Data acquisition was
30 performed using EPC-500 PowerChrom® software. After detection of ACh and Ch,
31 the dialysates were analyzed in the CMA-600 microdialysis analyser (CMA
32 Microdialysis AB, Stockholm, Sweden) to determine the concentrations of glucose
33 and lactate by an enzymatic reaction and colorimetric detection at 530 nm.
34
35

36
37 **Data analysis and statistical evaluation.** Data for the in vitro recovery of
38 microdialysis probes were given as means \pm standard deviation (SD). Concentrations
39 of ACh, Ch, energy metabolites and enzyme activities were expressed as means \pm
40 standard error of the mean (SEM) for the respective group with the number of
41 experiments indicated in figure legends. AChE and ChAT activity was analyzed with
42 Student's t-test using Prism 5 (GraphPad® Software, San Diego, USA). Two-way
43 ANOVA and Bonferroni post-test was used to analyze baseline concentrations of
44 ACh, Ch and manual ChI counting (with age and genotype as variables) and for
45 glucose and lactate levels (with challenge and genotype as variables). ACh and Ch
46 time courses as obtained by microdialysis were also analyzed using two-way ANOVA
47 for repeated measures (time and genotype as variables) and Bonferroni post-test.
48 Significance of data was assumed when statements could be made with 95%
49 confidence.
50
51

52 **Author Information**

53 **Corresponding Author**

*Mailing address: Department of Pharmacology, Goethe University of Frankfurt, Biocenter N260, Max-von-Laue-Str. 9, 60438 Frankfurt am Main, Germany. Fax: +49 69 798 29277. E-mail address: Klein@em.uni-frankfurt.de

Author Contributions

Microdialysis experiments and measurements of acetylcholine, choline, glucose and lactate were performed by MK. ChAT, HACU and AChE activity was measured by MK and BB. SF, KS and FT designed and performed experiments for ChAT-h- α -syn double labeling and ChI counting. GR, CRH, FT and CMW conceived the project. MK and JK wrote the paper and all authors reviewed the final manuscript. The authors gratefully acknowledge the technical support regarding HPLC measurements from Helene Lau and Mandy Magbagbeolu for expert histology.

Funding

This work was supported by TauRx Therapeutics Ltd., Singapore.

Notes

The authors declare no competing financial interest.

References

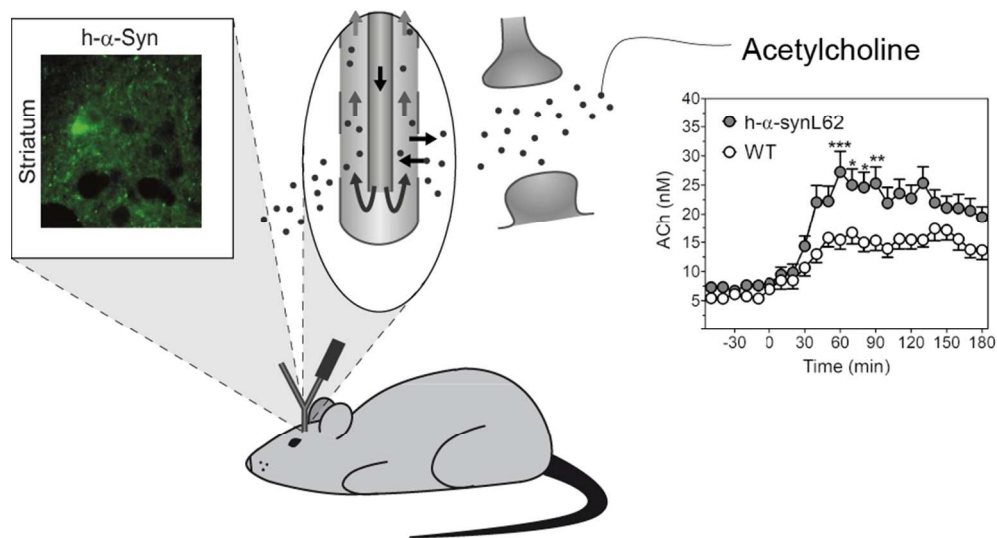
- (1) George, S.; Rey, N. L.; Reichenbach, N.; Steiner, J. A.; Brundin, P. α -Synuclein: The Long Distance Runner. *Brain Pathology*. 2013, Vol. 23, 350–357.
- (2) Jensen, P. H.; Nielsen, M. S.; Jakes, R.; Dotti, G.; Goedert, M. Binding of Alpha-Synuclein to Brain Vesicles Is Abolished by Familial Parkinsons-Disease Mutation. *J. Biol. Chem.* 1998, 273 (41), 26292–26294.
- (3) Burré, J.; Sharma, M.; Tsetsenis, T.; Buchman, V.; Etherton, M. R.; Südhof, T. C. Alpha-Synuclein Promotes SNARE-Complex Assembly in Vivo and in Vitro. *Science*. 2010, 329 (5999), 1663–1667.
- (4) Volpicelli-Daley, L. A. Effects of α -Synuclein on Axonal Transport. *Neurobiol. Dis.* 2017, 105, 321–327.
- (5) Wong, Y. C.; Krainc, D. α -Synuclein Toxicity in Neurodegeneration: Mechanism and Therapeutic Strategies. *Nat. Med.* 2017, 23 (2), 1–13.
- (6) Obeso, J. A.; Rodriguez-Oroz, M. C.; Rodriguez, M.; Lanciego, J. L.; Artieda, J.; Gonzalo, N.; Olanow, C. W. Pathophysiology of the Basal Ganglia in Parkinson's Disease. *Trends Neurosci.* 2000, 23 (10 Suppl), S8–S19.
- (7) Kawaguchi, Y.; Wilson, C. J.; Augood, S. J.; Emson, P. C. Striatal Interneurons: Chemical, Physiological and Morphological Characterization. *Trends in Neurosciences.* 1995, 527–535.
- (8) Zhou, F.-M.; Wilson, C. J.; Dani, J. A. Cholinergic Interneuron Characteristics and Nicotinic Properties in the Striatum. *J. Neurobiol.* 2002, 53 (4), 590–605.
- (9) Pisani, A.; Bernardi, G.; Ding, J.; Surmeier, D. J. Re-Emergence of Striatal Cholinergic Interneurons in Movement Disorders. *Trends Neurosci.* 2007, 30 (10), 545–553.
- (10) Smith, Y.; Villalba, R. Striatal and Extrastriatal Dopamine in the Basal Ganglia:

- 1
2
3 An Overview of Its Anatomical Organization in Normal and Parkinsonian
4 Brains. *Mov. Disord.* 2008, *23 Suppl 3*, S534-47.
- 5
6 (11) Bonsi, P.; Cuomo, D.; Martella, G.; Madeo, G.; Schirinzi, T.; Puglisi, F.;
7 Ponterio, G.; Pisani, A. Centrality of Striatal Cholinergic Transmission in Basal
8 Ganglia Function. *Front. Neuroanat.* 2011, *5*, 6.
- 9
10 (12) Koprach, J. B.; Kalia, L. V.; Brotchie, J. M. Animal Models of α -Synucleinopathy
11 for Parkinson Disease Drug Development. *Nature Reviews Neuroscience.*
12 2017, 515–529.
- 13
14 (13) Lundblad, M.; Decressac, M.; Mattsson, B.; Bjorklund, A. Impaired
15 Neurotransmission Caused by Overexpression of α -Synuclein in Nigral
16 Dopamine Neurons. *Proc. Natl. Acad. Sci.* 2012, *109* (9), 3213–3219.
- 17
18 (14) Daher, J. P. L.; Ying, M.; Banerjee, R.; McDonald, R. S.; Hahn, M. D.; Yang, L.;
19 Beal, M. F.; Thomas, B.; Dawson, V. L.; Dawson, T. M.; et al. Conditional
20 Transgenic Mice Expressing C-Terminally Truncated Human α -Synuclein
21 (ASyn119) Exhibit Reduced Striatal Dopamine without Loss of Nigrostriatal
22 Pathway Dopaminergic Neurons. *Mol. Neurodegener.* 2009, *4* (1).
- 23
24 (15) Lim, S. Y.; Fox, S. H.; Lang, A. E. Overview of the Extranigral Aspects of
25 Parkinson Disease. *Arch. Neurol.* 2009, *66* (2), 167–172.
- 26
27 (16) Frahm, S.; Melis, V.; Horsley, D.; Rickard, J. E.; Riedel, G.; Fadda, P.;
28 Scherma, M.; Harrington, C. R.; Wischik, C. M.; Theuring, F.; et al. Alpha-
29 Synuclein Transgenic Mice, h- α -SynL62, Display α -Syn Aggregation and a
30 Dopaminergic Phenotype Reminiscent of Parkinson's Disease. *Behav. Brain*
31 *Res.* 2018, *339* (August 2017), 153–168.
- 32
33 (17) Braak, H.; Del Tredici, K.; Rüb, U.; De Vos, R. A. I.; Jansen Steur, E. N. H.;
34 Braak, E. Staging of Brain Pathology Related to Sporadic Parkinson's Disease.
35 *Neurobiol. Aging* 2003, *24* (2), 197–211.
- 36
37 (18) Mattila, P. M.; Røyttä, M.; Lönnberg, P.; Marjamäki, P.; Helenius, H.; Rinne, J.
38 O. Choline Acetyltransferase Activity and Striatal Dopamine Receptors in
39 Parkinson's Disease in Relation to Cognitive Impairment. *Acta Neuropathol.*
40 2001, *102* (2), 160–166.
- 41
42 (19) Aldrin-Kirk, P.; Davidsson, M.; Holmqvist, S.; Li, J.-Y.; Björklund, T. Novel AAV-
43 Based Rat Model of Forebrain Synucleinopathy Shows Extensive Pathologies
44 and Progressive Loss of Cholinergic Interneurons. *PLoS One* 2014, *9* (7),
45 e100869.
- 46
47 (20) Jope, R. S. High Affinity Choline Transport and AcetylCoA Production in Brain
48 and Their Roles in the Regulation of Acetylcholine Synthesis. *Brain Research*
49 *Reviews.* 1979, 313–344.
- 50
51 (21) A.G. Black, S.; Jane Rylett, R. Choline Transporter CHT Regulation and
52 Function in Cholinergic Neurons. *Cent. Nerv. Syst. Agents Med. Chem.* 2012,
53 *12* (2), 114–121.
- 54
55 (22) Ferguson, S. M.; Savchenko, V.; Apparsundaram, S.; Zwick, M.; Wright, J.;
56 Heilman, C. J.; Yi, H.; Levey, A. I.; Blakely, R. D. Vesicular Localization and
57 Activity-Dependent Trafficking of Presynaptic Choline Transporters. *J.*
58 *Neurosci.* 2003, *23* (30), 9697–9709.
- 59
60

- 1
2
3 (23) Brandon, E. P.; Mellott, T.; Pizzo, D. P.; Coufal, N.; D'Amour, K. A.; Gobeske,
4 K.; Lortie, M.; López-Coviella, I.; Berse, B.; Thal, L. J.; et al. Choline
5 Transporter 1 Maintains Cholinergic Function in Choline Acetyltransferase
6 Haploinsufficiency. *J. Neurosci.* 2004, *24* (24), 5459–5466.
- 7
8 (24) Farrar, A. M.; Callahan, J. W.; Abercrombie, E. D. Reduced Striatal
9 Acetylcholine Efflux in the R6/2 Mouse Model of Huntington's Disease: An
10 Examination of the Role of Altered Inhibitory and Excitatory Mechanisms. *Exp.*
11 *Neurol.* 2011, *232* (2), 119–125.
- 12
13 (25) Mohr, F.; Krejci, E.; Zimmermann, M.; Klein, J. Dysfunctional Presynaptic M2
14 Receptors in the Presence of Chronically High Acetylcholine Levels: Data from
15 the PRiMA Knockout Mouse. *PLoS One* 2015, *10* (10), e0141136.
- 16
17 (26) Watanabe, H.; Shimizu, H.; Matsumoto, K. Acetylcholine Release Detected by
18 Trans-Striatal Dialysis in Freely Moving Rats Correlates with Spontaneous
19 Motor Activity. *Life Sci.* 1990, *47* (9), 829–832.
- 20
21 (27) Day, J.; Damsma, G.; Fibiger, H. C. Cholinergic Activity in the Rat
22 Hippocampus, Cortex and Striatum Correlates with Locomotor Activity: An in
23 Vivo Microdialysis Study. *Pharm. Biochem. Behav.* 1991, *38*, 723–729.
- 24
25 (28) Le Moine, C.; Normand, E.; Bloch, B. Phenotypical Characterization of the Rat
26 Striatal Neurons Expressing the D1 Dopamine Receptor Gene. *Proc. Natl.*
27 *Acad. Sci. U. S. A.* 1991, *88* (10), 4205–4209.
- 28
29 (29) Le Moine, C.; Tison, F.; Bloch, B. D2 Dopamine Receptor Gene Expression by
30 Cholinergic Neurons in the Rat Striatum. *Neurosci. Lett.* 1990, *117* (3), 248–
31 252.
- 32
33 (30) Maurice, N. D2 Dopamine Receptor-Mediated Modulation of Voltage-
34 Dependent Na⁺ Channels Reduces Autonomous Activity in Striatal Cholinergic
35 Interneurons. *J. Neurosci.* 2004, *24* (46), 10289–10301.
- 36
37 (31) Bertorelli, R.; Consolo, S. D1 and D2 Dopaminergic Regulation of Acetylcholine
38 Release from Striata of Freely Moving Rats. *J. Neurochem.* 1990, *54* (6),
39 2145–2148.
- 40
41 (32) Aosaki, T.; Kiuchi, K.; Kawaguchi, Y. Dopamine D1-like Receptor Activation
42 Excites Rat Striatal Large Spiny Neurons in Vitro. *J. Neurosci.* 1998, *18* (14),
43 5180–5190.
- 44
45 (33) Zhang, W.; Yamada, M.; Gomeza, J.; Basile, A. S.; Wess, J. Multiple
46 Muscarinic Acetylcholine Receptor Subtypes Modulate Striatal Dopamine
47 Release, as Studied with M1-M5 Muscarinic Receptor Knock-out Mice. *J.*
48 *Neurosci.* 2002, *22* (15), 6347–6352.
- 49
50 (34) Calabresi, P.; Centonze, D.; Gubellini, P.; Pisani, A.; Bernardi, G.
51 Acetylcholine-Mediated Modulation of Striatal Function. *Trends in*
52 *Neurosciences.* 2000, 120–126.
- 53
54 (35) Hartmann, J.; Kiewert, C.; Klein, J. Neurotransmitters and Energy Metabolites
55 in Amyloid-Bearing APP SWE X^{PS}SEN1dE9 Mouse Brain. *J. Pharmacol. Exp.*
56 *Ther.* 2010, *332* (2), 364–370.
- 57
58 (36) Ding, J.; Guzman, J. N.; Tkatch, T.; Chen, S.; Goldberg, J. A.; Ebert, P. J.;
59 Levitt, P.; Wilson, C. J.; Hamm, H. E.; Surmeier, D. J. RGS4-Dependent
60

- 1
2
3 Attenuation of M4 Autoreceptor Function in Striatal Cholinergic Interneurons
4 Following Dopamine Depletion. *Nat. Neurosci.* 2006, 9 (6), 832–842.
- 5
6 (37) Dobransky, T.; Rylett, R. J. A Model for Dynamic Regulation of Choline
7 Acetyltransferase by Phosphorylation. *J. Neurochem.* 2005, 95 (2), 305–313.
- 8
9 (38) Ostrerova, N.; Petrucelli, L.; Farrer, M.; Mehta, N.; Choi, P.; Hardy, J.; Wolozin,
10 B. Alpha-Synuclein Shares Physical and Functional Homology with 14-3-3
11 Proteins. *J. Neurosci.* 1999, 19 (14), 5782–5791.
- 12
13 (39) Stadler, H.; Lloyd, K. G.; Gadea-Ciria, M.; Bartholini, G. Enhanced Striatal
14 Acetylcholine Release by Chlorpromazine and Its Reversal by Apomorphine.
15 *Brain Res.* 1973, 55 (2), 476–480.
- 16
17 (40) Borghammer, P.; Chakravarty, M.; Jonsdottir, K. Y.; Sato, N.; Matsuda, H.; Ito,
18 K.; Arahata, Y.; Kato, T.; Gjedde, A. Cortical Hypometabolism and
19 Hypoperfusion in Parkinson's Disease Is Extensive: Probably Even at Early
20 Disease Stages. *Brain Struct. Funct.* 2010, 214 (4), 303–317.
- 21
22 (41) Pickrell, A. M.; Youle, R. J. The Roles of PINK1, Parkin, and Mitochondrial
23 Fidelity in Parkinson's Disease. *Neuron* 2015, 85 (2), 257–273.
- 24
25 (42) Ragozzino, M. E.; Unick, K. E.; Gold, P. E. Hippocampal Acetylcholine Release
26 during Memory Testing in Rats: Augmentation by Glucose. *Proc. Natl. Acad.
27 Sci. U. S. A.* 1996, 93 (10), 4693–4698.
- 28
29 (43) Messier, C.; Gagnon, M. Glucose Regulation and Cognitive Functions: Relation
30 to Alzheimer's Disease and Diabetes. *Behav. Brain Res.* 1996, 75 (1–2), 1–11.
- 31
32 (44) Schurr, A. Lactate: The Ultimate Cerebral Oxidative Energy Substrate? *J.
33 Cereb. Blood Flow Metab.* 2006, 26 (1), 142–152.
- 34
35 (45) Paxinos, G.; Franklin, K. B. The Mouse Brain in Stereotaxic Coordinates. 3rd
36 ed. 2001, 827–828.
- 37
38 (46) Fonnum, F. Radiochemical Micro Assays for the Determination of Choline
39 Acetyltransferase and Acetylcholinesterase Activities. *Biochem. J.* 1969, 115
40 (3), 465–472.
- 41
42 (47) Erb, C.; Troost, J.; Kopf, S.; Schmitt, U.; Löffelholz, K.; Soreq, H.; Klein, J.
43 Compensatory Mechanisms Enhance Hippocampal Acetylcholine Release in
44 Transgenic Mice Expressing Human Acetylcholinesterase. *J. Neurochem.*
45 2001, 77 (2), 638–646.
- 46
47 (48) Ellman, G. L.; Courtney, K. D.; Andres, V.; Featherstone, R. M. A New and
48 Rapid Colorimetric Determination of Acetylcholinesterase Activity. *Biochem.
49 Pharmacol.* 1961, 7 (2), 88–95.
- 50
51 (49) Zimmermann, M.; Westwell, M. S.; Greenfield, S. A. Impact of Detergents on
52 the Activity of Acetylcholinesterase and on the Effectiveness of Its Inhibitors.
53 *Biol. Chem.* 2009, 390 (1), 19–26.
- 54
55 (50) Bradford, M. M. A Rapid and Sensitive Method for the Quantitation of
56 Microgram Quantities of Protein Utilizing the Principle of Protein-Dye Binding.
57 *Anal. Biochem.* 1976, 72 (1–2), 248–254.
- 58
59 (51) Lietsche, J.; Gorke, J.; Hardt, S.; Karas, M.; Klein, J. Self-Built Microdialysis
60 Probes with Improved Recoveries of ATP and Neuropeptides. *J. Neurosci.*

1
2
3 *Methods* 2014, 237, 1–8.
4
5
6
7
8
9
10
11
12
13
14
15
16
17
18
19
20
21
22
23
24
25
26
27
28
29
30
31
32
33
34
35
36
37
38
39
40
41
42
43
44
45
46
47
48
49
50
51
52
53
54
55
56
57
58
59
60



For Table of Contents Use Only

81x43mm (300 x 300 DPI)